Letters in Applied NanoBioScience
Open-Access Journal (ISSN: 2284-6808)

*Article*
**Volume 12, Issue 2, 2023, 31**
https://doi.org/10.33263/LIANBS122.031

# Identification of Synthetic 2-Mercaptobenzimidazole Derivatives as Inhibitors of Spike Protein of SARS-CoV-2 by Virtual Screening

**Ricardo Silva Porto [1,*], Lucas Fernando de Lima Costa [1], Viviane Amaral Porto [2]**

[1] Institute of Chemistry and Biotechnology, Federal University of Alagoas, Maceió, Brazil
[2] Institute of Pharmaceutical Sciences, Federal University of Alagoas; Maceió, Brazil
* Correspondence: portto@iqb.ufal.br (R.S.P);

Scopus Author ID 8852139000
**Received: 17.11.2021; Accepted: 10.01.2022; Published: 14.03.2022**

**Abstract:** The severe acute respiratory syndrome coronavirus 2 (SARS-CoV-2) spread worldwide and caused the COVID-19 pandemic. Despite countless efforts in searching for repositioned drugs to treat this disease, the results are still modest. Thus, searching for new compounds as promising drugs to treat this disease is crucial. 2-Mercaptobenzimidazole, a scaffold found in many biologically relevant compounds, has been extensively studied due to its range of biological activities. Using *in silico* tools, this study aimed to identify 2-mercaptobenzimidazole derivatives as potential drugs to inhibit SARS-CoV-2 infection by blocking spike protein – human angiotensin-converting (hACE2) enzyme interaction. 61 compounds were screened to evaluate their absorption, distribution, metabolism, and excretion (ADME) properties. The compounds that did not violate any Lipinski or Veber rules were subjected to molecular docking interactions to verify their ability to inhibit spike glycoprotein from binding to the hACE2 enzyme. The docking scores for these compounds were superior to the antiviral drugs Remdesivir and Umifenovir, proven to be potential drugs against COVID-19. Furthermore, 2-mercaptobenzimidazole derivatives have been shown to interfere in amino acids involved in key contact sites between SARS-CoV-2-CTD and hACE2 subdomain I. Finally, some toxicological properties were predicted, and the compounds exhibited few (or none) alerts for toxic endpoints as well as low predicted acute oral toxicity ($LD_{50}$). In this way, the results presented in this work should contribute to discovering new drugs against SARS-CoV-2.

**Keywords:** 2-mercaptobenzimidazole; SARS-CoV-2; spike protein; virtual screening.



## 1. Introduction

The COVID-19 pandemic, caused by the SARS-CoV-2 viruses, continues to affect people's wellbeing and lifestyle worldwide [1, 2]. Thus, it is now known that pre-existing health conditions such as high blood pressure, obesity, and diabetes can enhance the severity of the disease and the individual's susceptibility to infection [3]. While worldwide vaccination is still a challenge, several efforts are underway, especially in drug discovery, which aims the disease's control, given its dire impact on people's lives [4, 5]. In this scenario, there is a need to identify novel drug lead compounds for treating COVID-19.

The SARS-CoV-2 can access the respiratory system after the airborne viral particles inhalation. Upon entering the airways, the virus particles encounter respiratory epithelium cells in the trachea and lungs [6]. The virus's surface contains spike proteins (S), membrane proteins,

and envelope proteins. The SARS-CoV-2 virus mechanism acts through its spike proteins, recognizing a functional receptor on cell surfaces known as human Angiotensin-converting enzyme 2 (hACE2), which is highly expressed in the heart and kidneys lungs and shed into the plasma [7]. Once bound to hACE2, the spike protein cannot open, close, or bend freely, remaining locked in place. Another cell surface protein called transmembrane protease serine 2 (TMPRSS2) cuts the spike protein in a specific location [8]. The SARS-CoV-2 spike protein would, in most cases, be cleaved by the host proteases into the S1 and S2 subunits [8, 9]. These segments of spike protein fall away and expose previously hidden parts.

As a result, the spike protein starts a process of conformational changes to insert itself into the membrane receptor and access the cell. After binding, the spike protein suffers another change, bending back, taking together cell and virus membrane in a fusion process. After fusion, the virus RNA is released into the host cell, hijacking the cell's machinery to produce more virus particles. The C-terminal domain of the SARS-CoV-2 S1 subunit (SARS-CoV-2-CTD) is where the virus binds to the hACE2 enzyme on the host cell's surface, enabling it to fuse with the cell [9]. SARS-CoV-2-CTD forms more atomic interactions with hACE2 than other coronaviruses, which correlates with data showing a higher affinity for receptor binding. Thus, blocking the binding of the spike protein to ACE2 is an efficient approach to inhibit SARS-CoV-2 infection of target cells [10]. Diverse studies have described and identified potential compounds as drugs that can inhibit spike protein [11-16].

2-mercaptobenzimidazole 1 (2-MBI, figure 1) is an aromatic heterocyclic ring found in many biologically relevant synthetic compounds and natural products [17-19]. 2-MBI consists of a bicyclic structure in which the imidazole is fused to a benzene ring, having an exocyclic sulfur atom in position 2 [20]. The biological activities of 2-MBI derivatives are widely explored in literature and include anti-inflammatory [21], anticonvulsant [22], antidiabetic [23], anti-ulcer [24], anticancer [25], and antimicrobial [26]. Among the drugs containing the 2-MBI nucleus found on the market, we can mention the medicines used to treat ulcers, such as omeprazole, pantoprazole, and rabeprazole [27]. These drugs inhibit the proton pump irreversibly in stomach tissue cells, where acidic secretion is produced for food digestion. The enzyme inhibition occurs through a covalent bond to the specific site of the enzyme in the cell membrane [28]. According to the mechanism of action, mercaptobenzimidazole rings are essential for the drug's activity. Furthermore, several 5-membered aromatic systems with 2 and 3 heteroatoms in symmetrical positions have shown structural importance in medicinal chemistry due to their remarkable properties in terms of binding mechanisms and enzyme inhibition [29, 30]. Therefore, given the significant biological potential of 2-MBI, this work aimed to report the identification of synthetic compounds that contain the 2-MBI scaffold as promising drugs to inhibit spike protein binding to the cell membrane and treat COVID-19.

As tools to perform virtual screening of compounds, *in silico* ADMET predictions were applied to analyze the pharmacokinetic profile and toxicity of sixty-one 2-MBI derivatives. Furthermore, molecular docking was performed in order to reveal the most promising 2-MBI derivatives as inhibitors of the spike protein of the SARS-CoV-2 virus.

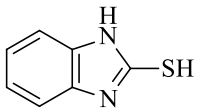


**Figure 1.** 2-mercaptobenzimidazole (2-MBI).

## 2. Materials and Methods

### *2.1. Selection and preparation of ligands.*

The chemical structure accessing of the 2-MBI derivatives was performed using the SciFinder database (https://scifinder.cas.org). Only compounds with biological activity already reported in the literature were chosen for analysis. Sixty-one compounds were prepared in this stage. The chemical structure of compounds was built using Chemdraw Ultra version 12.0 [31]. Three-dimensional structures were generated by Chem3D and optimized by MMFF94s force field [32], implemented in the freeware Avogadro® version 1.2.0 [33].

### *2.2. ADME/T prediction of ligands.*

*In silico* ADME/T profile is a valuable tool to predict drug candidates' pharmacological and toxicological properties [34-36]. Physicochemical and pharmacokinetic properties such as molecular weight, H-bond donors, H-bond acceptors, consensus Log *P*, number of rotatable bonds, and topological polar surface area (TPSA) were performed using SwissADME [37]. The toxicological profile of the compounds was evaluated through the freely accessible ProTox-II online application [38]. Canonical smiles, generated in Chemdraw, were used for ADMET analysis.

### *2.3. Molecular docking protocol.*

The structure of SARS-CoV-2 Spike protein, retrieved from Protein Data Bank (PDB ID: 6LZG), was used as a template for docking calculations. GOLD, version 2020.3.0 [39], a docking tool based on a genetic algorithm (GA), was chosen to study the protein target. Gold has proven success in virtual screening, lead optimization, and identifying the correct binding mode of potential drug candidates [40-42]. Grid parameter configuration file was created for Gold with dimensions of (X = −36.0, Y = 20.0, Z = 7.0). 10 GA runs were performed for each ligand. The highest scored docking poses were analyzed using Hermes, and the distances and angles were measured using Discovery Studio Visualizer [43].

## 3. Results and Discussion

### *3.1. In silico ADME properties.*

To be effective, a drug ought to reach its target. Therefore the compound with the best binding interactions is not necessarily the best potential drug. The Lipinski rule supports the oral bioavailability, which is an essential characteristic of a druggable compound and a crucial factor in optimizing bioactive molecules as therapeutic agents [44]. We were careful to select compounds with no violations of the Lipinski rule, which states that drug-likeness compounds must have HBD (hydrogen bond donor) less than 5, HBA (hydrogen bond acceptor) less than 10, molecular weight not greater than 500 Da, and cLOGP ≤ 5. The work developed by Veber [45] showed that molecular flexibility plays an essential role in oral bioavailability. In other words, the more flexible the compound, the less likely it is to be orally active. One way to measure flexibility is to count the number of rotatable bonds (NRB), which results in different conformations. Veber's studies also demonstrated the topological polar surface area (TPSA). The TPSA is defined as the sum of all polar atoms, primarily oxygen and nitrogen, including their attached hydrogen. Moreover, it is considered a crucial physicochemical parameter in

predicting the drug's distribution [45]. These findings led to the following parameters for predicting acceptable oral activity: a polar surface area ≤140 Å$^2$ and ≤10 rotatable bonds. From the 61 compounds submitted to the SwissAdme server, 22 presented at least one Lipinski and/or Veber violations and were, thus, excluded from further studies (Table S2). The molecular weight was found to be > 500 in 14 compounds, and it was also the number of compounds with cLOGP > 5. 13 compounds showed NRB > 10, and 8 compounds presented TPSA > 140 Å$^2$. All the compounds showed HBD and HBA less than 5 and 10, respectively.

*3.2. Validation of the accuracy and performance of gold.*

The docking accuracy can be evaluated by re-docking the native ligand to inspect how close the best-scoring pose reproduces the crystallographic binding mode.

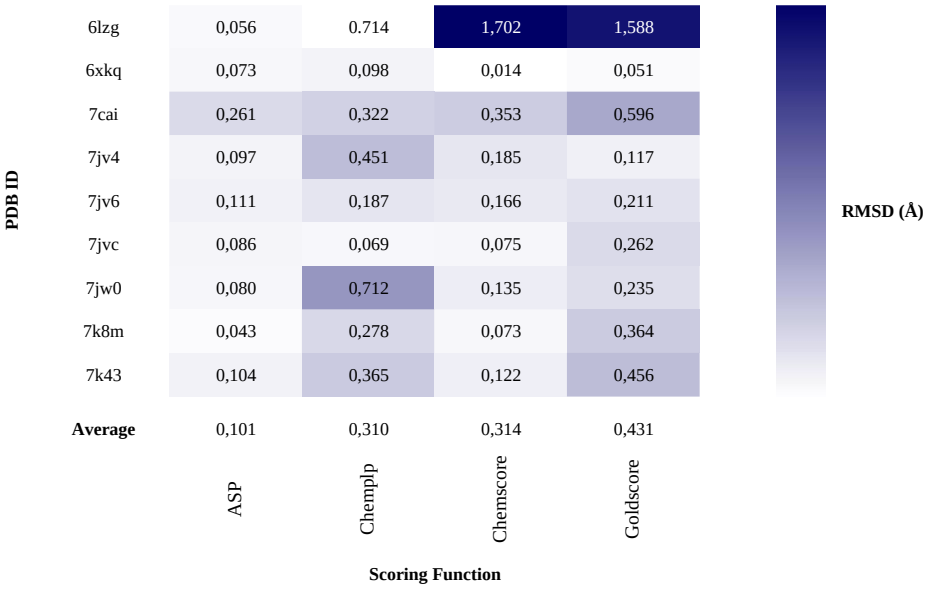


**Figure 2**. Re-docking for co-crystallized ligands with different co-crystal proteins; each row represents a structure, and the columns identify the scoring functions. Values shown are the RMSD for the best-scoring docked pose to the crystal structure pose. The RMSD values are highlighted and depicted using a colorimetric scale from white to dark blue for values from 0 to 1.702 Å.

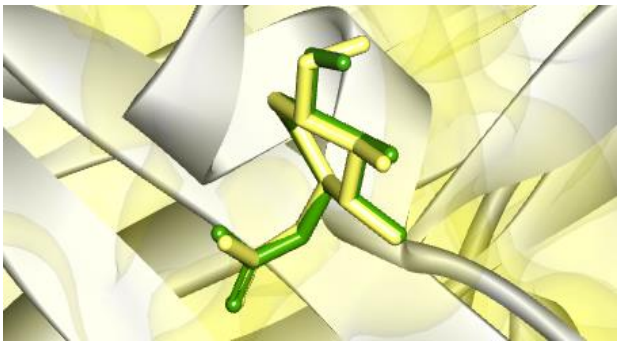

**Figure 3**. Overlays of crystallographic ligand pose NAG (in green), with the calculated pose (in yellow).

Root mean squared deviations (RMSD) ≤ 2.0 Å from co-crystallized ligand are acceptable values for docking validation. RMSD was calculated and summarized as a heat map (Figure 2). The results showed that, among the four scoring functions (ASP, Chemplp, Chemscore, and GoldScore), the eleven PDB structures of SARS-CoV-2 spike glycoprotein tested exhibited RMSD values ≤ 2.0 Å. ASP reproduced native ligands more accurately (RMSD ≤ 0.261 Å), displaying the lowest average RMSD and 6LZG, the protein with the lowest RMSD value (0.056 Å). Figure 3 shows the overlay of the co-crystallized native ligand

pose with the calculated pose for the chosen score function (ASP) and protein (6LZG) to perform the molecular docking for the selected compounds.

*3.3. Molecular docking calculations.*

As far as we know, there are no studies in the literature involving the interaction of 2-MBI derivatives with the SARS-CoV-2 spike protein. Interestingly, a recent paper has described the molecular docking of 2-MBI itself with the SARS-CoV-2 main protease [46]. Thus, the present study aims to verify how 2-MBI derivatives might bind in the active site of the coronavirus spike protein and change the way it interacts with human Angiotensin-converting enzyme 2, resulting in biological activity. We chose the grid box tridimensional parameters based on Wang's study [9], which determined the key region responsible for interacting with the receptor in the SARS-CoV-2 crystal structure. According to these authors, the SARS-CoV-2 Carbon terminal domain (SARS-CoV-2 CTD) can bind to hACE2. The CTD has a key role in receptor binding and is an ideal target for vaccine or drug development. The 39 compounds that presented good drug-likeness properties were subjected to molecular docking against the C-terminal domain of the Spike S1 subunit and compared with known inhibitors. Table S2 shows the docking scores for these compounds obtained in the Gold software. Compounds ***13***, ***2***, and ***17*** exhibited the highest docking scores, ranging from 49.00 to 47.94. Subsequently, compounds ***14***, ***1***, ***20***, and ***22*** completed the ranking of the seven top-scored compounds, with docking scores varying from 47.69 to 40.10. In general, 2-MBI derivatives showed superior scores than antiviral drugs Remedisivir and Umefinovir [47]. Remdesivir proved to be a potent drug against COVID-19 [48]. All these results are summarized in Table 1 and the chemical structure of the title compounds.

**Table 1.** Calculated docking (ASP.Fitness) score for 2-MBI derivatives with SARS-CoV-2 spike protein.

| Compound | Structure | ASP.Fitness score |
|---|---|---|
| **13** | 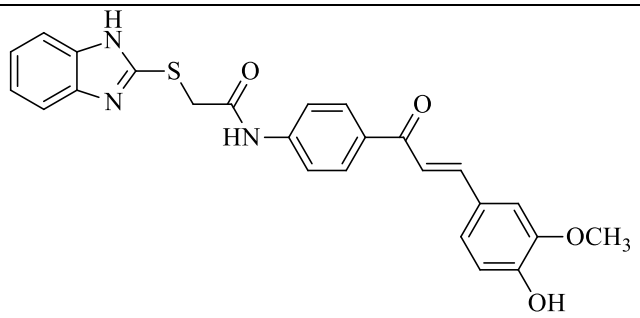 | 49.00 |
| **2** | 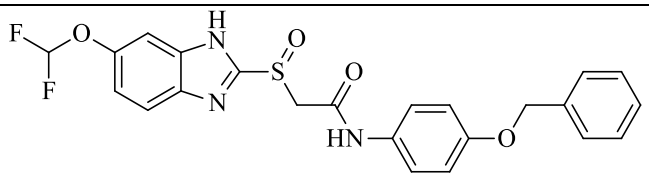 | 48.64 |
| **17** | 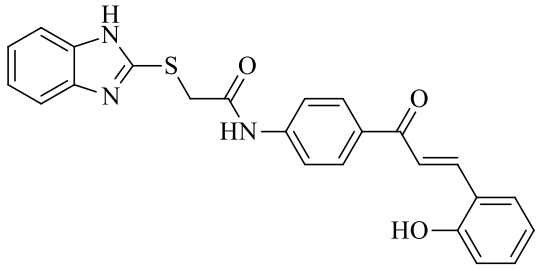 | 47.94 |

| Compound | Structure | ASP.Fitness score |
|---|---|---|
| **14** | 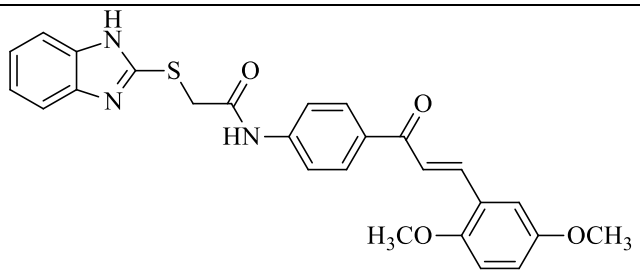 | 47.69 |
| **1** | 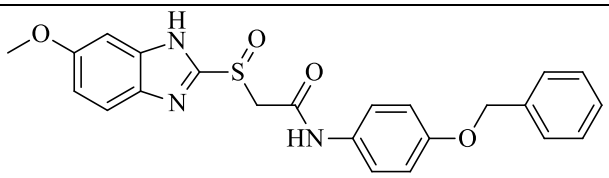 | 45.33 |
| **20** | 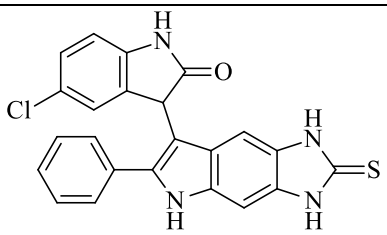 | 40.39 |
| **22** | 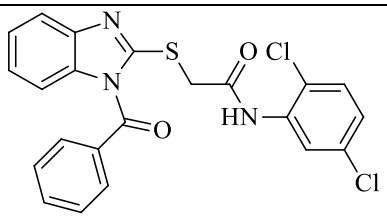 | 40.10 |
| | Remdesivir [ 47, 48] | 36.37 |
| | Umifenovir [ 47] | 33.30 |

Figure 4 shows the docking structure of ACE2 bound with spike protein fragment in the presence of 2-MBI **13**, inserted in the SARS-CoV-2 CTD protein's pocket. Figure 5 illustrates the detailed interactions of compounds **13**, **2**, and **17** with spike protein. We can observe from the figure that compounds **13** and **2** interact through H-bonding with ARG403, ASP38, and GLN493, whereas binds with hydrophobic interactions with TYR449. Compound **2** interacts with GLY496, PHE390, and LYS353 through H-bonding and hydrophobic interactions with ASN33, GLU35, GLU37, HIS34, PRO389, and TYR449. Moreover, compound **13** presents H-bonding interaction with ASN33 and hydrophobic interaction with HIS34. Finally, compound **17** interacts by H-bonding with TYR505 and hydrophobic interactions with ARG393 and GLU37.

As previously described by Wang *et al*., [9], key contact sites between SARS-CoV-2-CTD and hACE2 subdomain I involve amino acids such as GLY496, HIS34 TYR449. Hence, *in silico* molecular docking results revealed that synthetic 2-MBI derivatives have proven as potential compounds to inhibit the new coronavirus since they can potentially interfere in these contacts and prevent virus activity. Furthermore, these compounds can be easily obtained from an inexpensive starting material in short synthetic routes, making them promising candidate drugs to treat COVID-19.

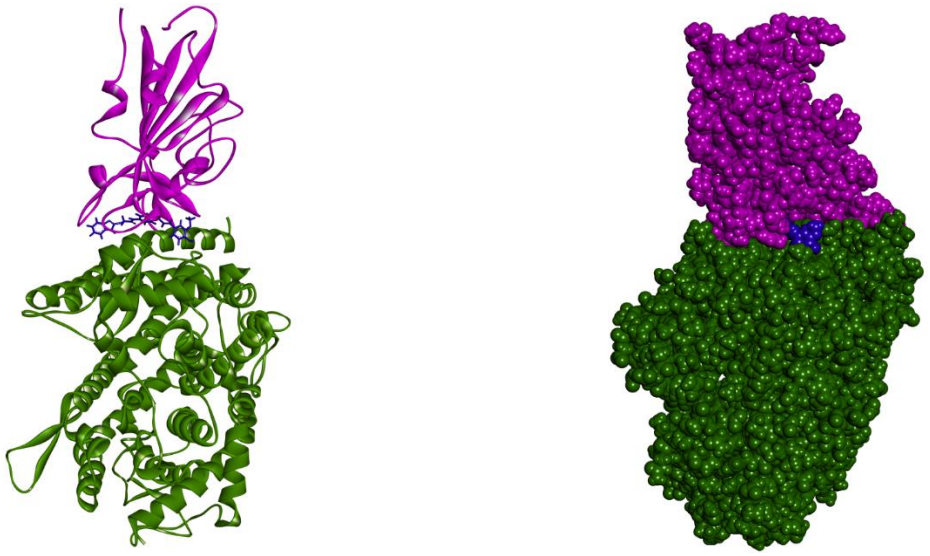

**a** **b**

**Figure 4**. Docking structure of ACE2 (in green) bound with spike protein fragment (in pink) in the presence of 13 (blue); (**a**) ribbon representation; (**b**) hydrophobic surface**.**

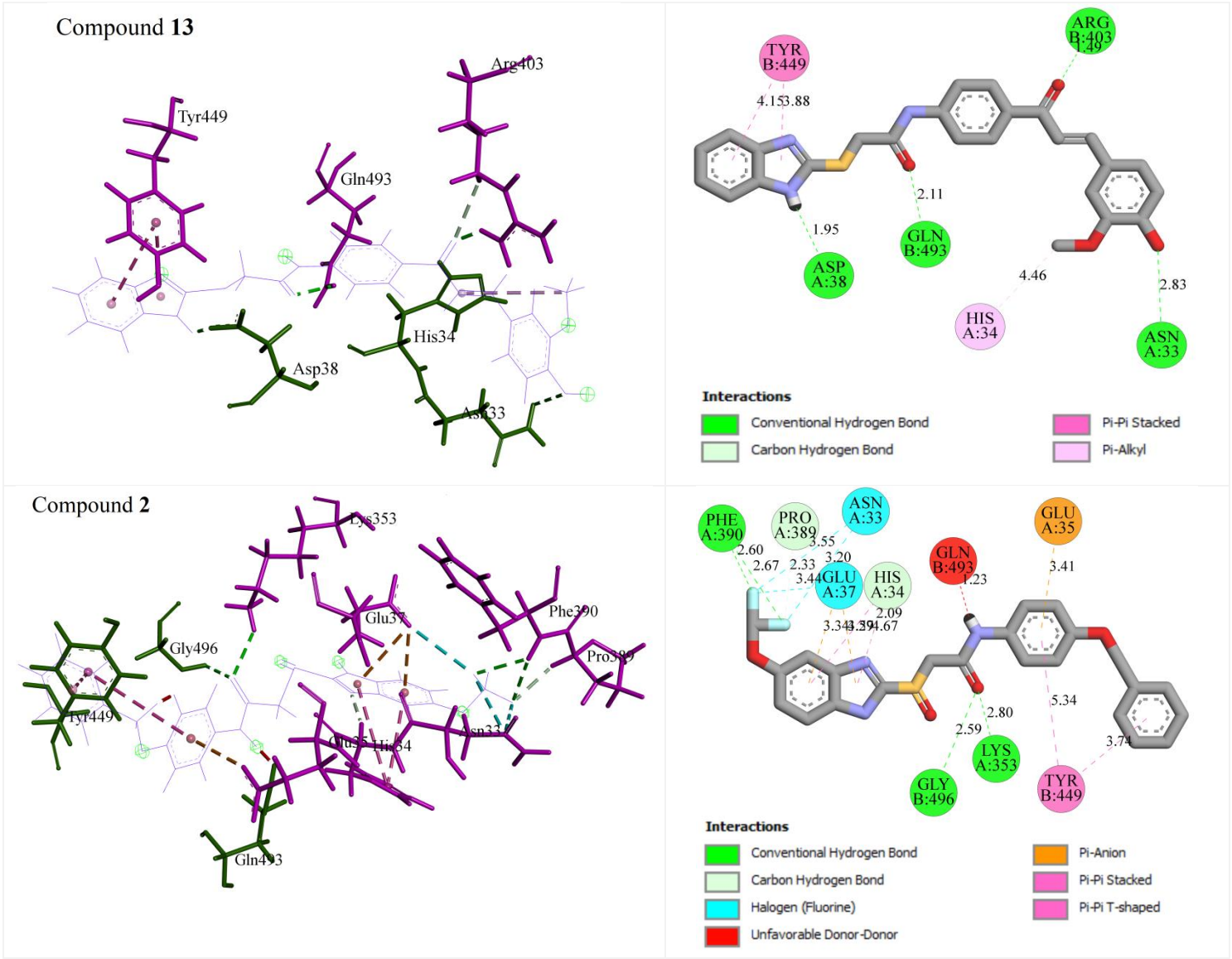

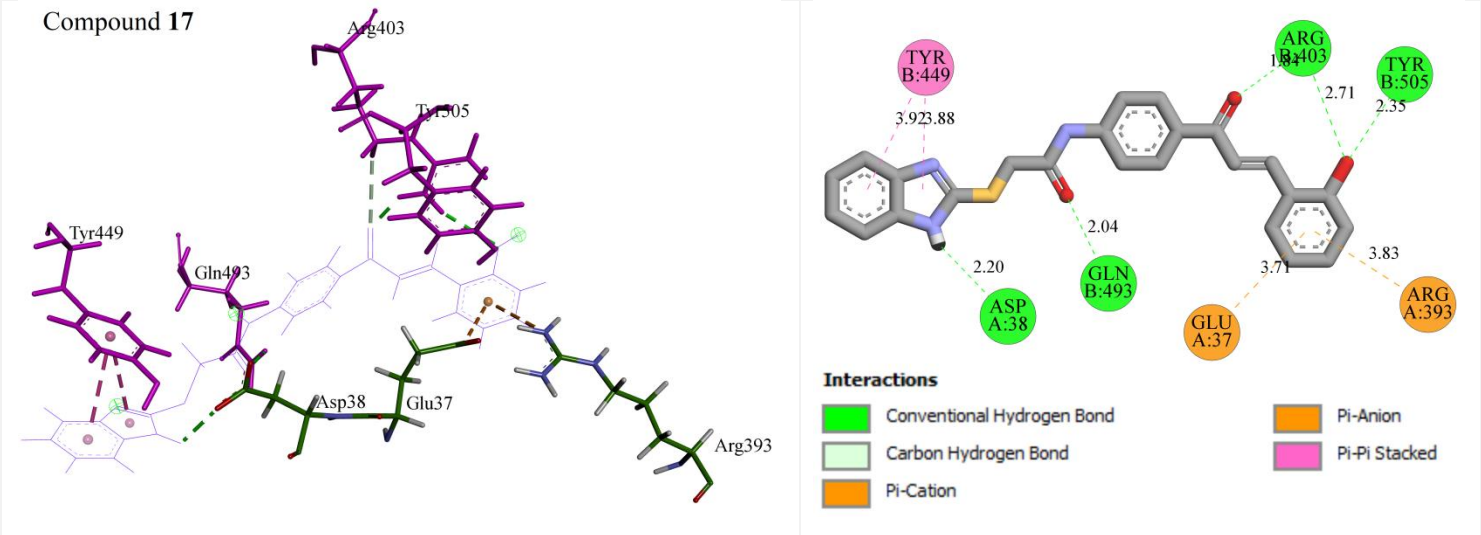


**Figure 5.** Interactions of the active spike protein site with compounds **13**, **2,** and **17.**

*3.4. Toxicological properties.*

The toxicological parameters for the best-docked 2-MBI derivatives with toxicity alert results are shown in Table 2. By applying the ProTox-II tool, toxicity endpoints such as carcinogenicity, immunotoxicity, mutagenicity, cytotoxicity, as well as $LD_{50}$ were predicted. The following paragraphs will detail dysfunctions associated with a specific substance's toxicity.

Alerts for carcinogenicity are defined as molecular functional groups or substructures linked to compounds' carcinogenic activity. Thus, they identify the main chemical classes capable of causing cancer [49]. Since DNA modification is the foremost step in the mechanism of action of many carcinogens (i.e., so-called genotoxic carcinogens), alerts relating to these classes of carcinogens are also valid for the mutagenicity endpoint. The Ames test has been widely used to identify mutagens among pure substances, complex mixtures, and environmental samples [50-52]. It is characterized by Salmonella typhimurium indicator lines sensitive to substances capable of inducing different types of mutations. A positive test indicates that the compound is potentially mutagenic and may be a carcinogenic agent.

Immunotoxicity is related to the harmful action of various chemical and physical agents on the immune system [53]. For example, exposure to potential immunotoxic compounds is known to cause disturbances in the immune system since it impairs the proliferation of T and B lymphocytes, which contributes to the increase in the risk of opportunistic infections compromising the immune systems.

Cytotoxicity is the intrinsic ability of a given substance to promote metabolic change in cultured cells, which may or may not lead to cell death [54]. Thus, cytotoxic substances can decrease a tissue's self-renewal capacity or cause its degeneration by cell death. In turn, this death can occur by different types, grouped into two morphological classes, necrosis and apoptosis.

The selected compounds showed few toxicity alerts (0 or 1). Compounds **13** and **14** presented an alert immunotoxicity, and compound **20** presented an alert for carcinogenicity. All other compounds did not show any toxicity effects. In addition, all the compounds showed a low predicted oral acute toxicity class ($LD_{50}$), which places them as class 4 in the Globally Harmonized System (GHS) classification for acute oral toxicity.

**Table 2.** Toxicological properties for the selected compounds.

| Compound | Carcinogenicity | Immunotoxicity | Mutagenicity | Cytotoxicity | $LD_{50}$ (mg/kg) | Toxicity Class | Alerts |
|---|---|---|---|---|---|---|---|
| **13** | Inactive | **Active** | Inactive | Inactive | 2000 | 4 | **1** |
| **2** | Inactive | Inactive | Inactive | Inactive | 500 | 4 | **0** |
| **17** | Inactive | Inactive | Inactive | Inactive | 500 | 4 | **0** |
| **14** | Inactive | **Active** | Inactive | Inactive | 500 | 4 | **1** |
| **1** | Inactive | Inactive | Inactive | Inactive | 500 | 4 | **0** |
| **20** | **Active** | Inactive | Inactive | Inactive | 2000 | 4 | **1** |
| **22** | Inactive | Inactive | Inactive | Inactive | 500 | 4 | **0** |

## 4. Conclusions

The 2-mercaptobenzimidazole represents a privileged scaffold demonstrating many relevant pharmacological activities. This study performed a virtual screening through ADMET predictions and molecular docking. From the 61 compounds evaluated, 22 were preliminarily filtered out for not presenting satisfactory pharmacokinetic properties. The 39 remaining compounds were subjected to molecular docking studies and ranked in binding affinities through ASP.Fitness score. The results revealed that 2-MBI derivatives showed better binding affinity in the protein spike site than Remdesivir and Umifenovir. These 2 antiviral drugs previously described as promising inhibitors of spike glycoprotein. Furthermore, Remdesivir, the only current drug used to treat the new coronavirus, has a complex structure, resulting in highly costly treatment. In this way, 2-MBI derivatives rise as low-cost antiviral alternatives in treating COVID-19, presenting good synthetic accessibility and supporting further research in drug design. Finally, good pharmacokinetics and low toxicology make the mentioned compounds promising drugs for oral treatment.

## Funding

This research received no external funding.

## Acknowledgments

Declared none.

## Conflicts of Interest

The authors declare no conflict of interest.

## References

1. Phiri, P.; Ramakrishnan, R.; Rathod, S.; Elliot, K.; Thayanandan, T.; Sandle, N.; Haque, N.; Chau, S.W.H.; Wong, O.W.H.; Chan, S.S.M.; Wong, E.K.Y.; Raymont, V.; Au-Yeung, S.K.; Kingdon, D. Delanerolle, G. An evaluation of the mental health impact of SARS-CoV-2 on patients, general public and healthcare professionals: A systematic review and meta-analysis. *EClinicalMedicine* **2021**, *34*, 100806, https://doi.org/10.1016/j.eclinm.2021.100806.
2. Reese, G.; Hamann, K.R.; Heidbreder, L.M.; Loy, L.S.; Menzel, C.; Neubert, S.; Troger, J.; Wullenkord, M.C. SARS-Cov-2 and environmental protection: A collective psychology agenda for environmental psychology research. *Journal of environmental psychology* **2020**, *70*, 101444, https://doi.org/10.1016/j.jenvp.2020.1014444.
3. Ejaz, H.; Alsrhani, A.; Zafar, A.; Javed, H.; Junaid, K.; Abdalla, A.E.; Abosalif, K.O.A.; Ahmed, Z.; Younas, S. COVID-19 and comorbidities: Deleterious impact on infected patients. *Journal of infection and public health* **2020**, *13*, 1833-1839, https://doi.org/10.1016/j.jiph.2020.07.0144.

4. Mohamed, K.; Yazdanpanah, N.; Saghazadeh, A; Rezaei, N. Computational drug discovery and repurposing for the treatment of COVID-19: a systematic review. *Bioorganic chemistry* **2021**, *106*, 104490, https://doi.org/10.1016/j.bioorg.2020.1044900.
5. Porto, V.A; Porto, R.S. *In silico* studies of novel synthetic compounds as potential drugs to inhibit coronavirus (SARS-CoV-2): A systematic review. *Biointerface Res. Appl. Chem* **2022**, *12*, 4293-4306, https://doi.org/10.33263/BRIAC124.429343066.
6. Zuo, Y.Y.; Uspal, W.E.; Wei, T. Airborne transmission of COVID-19: aerosol dispersion, lung deposition, and virus-receptor interactions. *ACS nano* **2020**, *14*, 16502-16524, https://doi.org/10.1021/acsnano.0c08484.
7. Beyerstedt, S.; Casaro, E.B.; Rangel, É.B. COVID-19: angiotensin-converting enzyme 2 (ACE2) expression and tissue susceptibility to SARS-CoV-2 infection. *European Journal of Clinical Microbiology & Infectious Diseases* **2021**, *40*, 905-919, https://doi.org/10.1007/s10096-020-04138-6.
8. Hoffmann, M.; Pöhlmann, S. How SARS-CoV-2 makes the cut. *Nature Microbiology* **2021**, *6*, 828-829, https://doi.org/10.1038/s41564-021-00931-x.
9. Wang, Q.; Zhang, Y.; Wu, L.; Niu, S.; Song, C.; Zhang, Z.; Lu, G.; Qiao, C.; Hu, Y.; Yuen, K. Y.; Wang, Q.; Zhou, H.; Yan, J.; Qi, J. Structural and functional basis of SARS-CoV-2 entry by using human ACE2. *Cell* **2020**, *181*, 894-904, https://doi.org/10.1016/j.cell.2020.03.045.
10. Wu, Y.; Li, C.; Xia, S.; Tian, X.; Kong, Y.; Wang, Z.; Gu, C.; Zhang, R.; Tu, C.; Xie, Y.; Yang, Z.; Lu, L.; Jiang, S,; Ying, T. Identification of human single-domain antibodies against SARS-CoV-2. *Cell host & microbe* **2020**, *27*, 891-898, https://doi.org/10.1016/j.chom.2020.04.023.
11. Baig, M.S.; Alagumuthu, M.; Rajpoot, S.; Saqib, U. Identification of a potential peptide inhibitor of SARS-CoV-2 targeting its entry into the host cells. *Drugs in R&D* **2020**, *20*, 161-169, https://dx.doi.org/10.1007%2Fs40268-020-00312-5.
12. Pandey, P.; Rane, J.S.; Chatterjee, A.; Kumar, A.; Khan, R.; Prakash, A.; Ray, S. Targeting SARS-CoV-2 spike protein of COVID-19 with naturally occurring phytochemicals: an *in silico* study for drug development. *Journal of biomolecular Structure and Dynamics* **2021**, *39*, 6306-6316, https://doi.org/10.1080/07391102.2020.1796811.
13. Pirolli, D.; Righino, B.; De Rosa, M.C. Targeting SARS-CoV-2 Spike Protein/ACE2 Protein-Protein Interactions: a Computational Study. *Molecular informatics* **2021**, *40*, 2060080, https://doi.org/10.1002/minf.202060080.
14. Pandey, P.; Khan, F.; Rana, A.K.; Srivastava, Y.; Jha, S.K.; Jha, N.K. A drug repurposing approach towards elucidating the potential of flavonoids as COVID-19 spike protein inhibitors. *Biointerface Res. Appl. Chem* **2021**, *11*, 8482-8501, https://doi.org/10.33263/BRIAC111.84828501.
15. Prasanth, D.S.N.B.K.; Murahari, M.; Chandramohan, V.; Panda, S.P.; Atmakuri, L.R.; Guntupalli, C. *In silico* identification of potential inhibitors from *Cinnamon* against main protease and spike glycoprotein of SARSCoV-2. *Journal of Biomolecular Structure and Dynamics* **2020**, *39*, 4618-4632, https://doi.org/10.1080/07391102.2020.1779129.
16. Awad, I.E.; Abu-Saleh, A.A.A.A.; Sharma, S.; Yadav, A.; Poirier, R.A. High-throughput virtual screening of drug databanks for potential inhibitors of SARS-CoV-2 spike glycoprotein. *Journal of Biomolecular Structure and Dynamics* **2020**, 1-14, https://doi.org/10.1080/07391102.2020.1835721.
17. Azam, M.A.; Suresh, B. Biological activities of 2-mercaptobenzothiazole derivatives: a review. *Scientia pharmaceutica* **2012**, *80*, 789-824, https://doi.org/10.3797/scipharm.1204-27.
18. de Assis, J.V.; Couri, M.R.C.; Porto, R.S.; de Almeida, W.B.; dos Santos, L.H.; Diniz, R.; de Almeida, M.V. Synthesis of Mercaptobenzothiazole and Mercaptobenzimidazole Condensed with Inositol Derivatives. *Journal of Heterocyclic Chemistry* **2013**, *50*, E142-E147, https://doi.org/10.1002/jhet.1096.
19. Sharma, P. K. A review: Antimicrobial agents based on nitrogen and sulfur containing heterocycles. *Asian J. Pharm. Clin. Res* **2017**, *10*, 47-49, http://dx.doi.org/10.22159/ajpcr.2017.v10i2.15673.
20. Silva, A.L.; da Silva, M.D.R. Energetic, structural and tautomeric analysis of 2-mercaptobenzimidazole. *Journal of Thermal Analysis and Calorimetry* **2017**, *129*, 1679-1688, https://doi.org/10.1007/s10973-017-6353-x.
21. Khan, M. T.; Nadeem, H.; Khan, A.U.; Abbas, M.; Arif, M.; Malik, N.S.; Malik, Z.; Javed, I. Amino acid conjugates of 2-mercaptobenzimidazole provide better anti-inflammatory pharmacology and improved toxicity profile. *Drug Development Research* **2020**, *81*,1057-1072, https://doi.org/10.1002/ddr.21728.
22. Anandarajagopal, K.; Tiwari, R.N.; Bothara, K.G.; Sunilson, J.A.J.; Dineshkumar, C.; Promwichit, P. 2-Mercaptobenzimidazole derivatives: synthesis and anticonvulsant activity. *Advances in Applied Science*

*Research* **2010**, *1*, 132-138, https://www.imedpub.com/articles/2mercaptobenzimidazole-derivatives-synthesis-andanticonvulsant-activity.pdf.
23. Ali, M.; Ali, S.; Khan, M.; Rashid, U.; Ahmad, M.; Khan, A.; Al-Harrasi, A.; Ullah, F.; Latif, A. Synthesis, biological activities, and molecular docking studies of 2-mercaptobenzimidazole based derivatives. *Bioorganic chemistry* **2018**, *80*, 472-479, https://doi.org/10.1016/j.bioorg.2018.06.032.
24. Noor, A.; Qazi, N.G.; Nadeem, H.; Khan, A.U.; Paracha, R.Z.; Ali, F.; Saeed, A. Synthesis, characterization, anti-ulcer action and molecular docking evaluation of novel benzimidazole-pyrazole hybrids. *Chemistry Central Journal* **2017**, *11*, 85, https://doi.org/10.1186/s13065-017-0314-0.
25. Tahlan, S.; Narasimhan, B.; Lim, S.M.; Ramasamy, K.; Mani, V. Shah, S.A. 2-Mercaptobenzimidazole Schiff bases: design, synthesis, antimicrobial studies and anticancer activity on HCT-116 cell line. *Mini reviews in medicinal chemistry* **2019**, *19*, 1080-1092, http://dx.doi.org/10.2174/1389557518666181009151008.
26. Yaseen, G.; Sudhakar, J. Design, synthesis and antimicrobial activity of 2-mercaptobenzimidazole derivatives. *International Journal of Pharma and Bio Sciences* **2010**, *1*, 281-286.
27. Ochoa, D.; Román, M.; Cabaleiro, T.; Saiz-Rodríguez, M.; Mejía, G.; Abad-Santos, F. Effect of food on the pharmacokinetics of omeprazole, pantoprazole and rabeprazole. *BMC Pharmacology and Toxicology* **2020**, *21*, 54, https://doi.org/10.1186/s40360-020-00433-2.
28 Vanderhoff, M.D.; Tahboub, R.M. Proton pump inhibitors: an update. *Am Fam Physician* **2002**, *66*, 273-280.
29. Hosamani, K.M.; Shingalapur, R.V. Synthesis of 2-Mercaptobenzimidazole Derivatives as Potential Anti-microbial and Cytotoxic Agents. *Archiv der Pharmazie* **2011**, *344*, 311-319, https://doi.org/10.1002/ardp.200900291.
30. Tomei, L.; Altamura, S.; Bartholomew, L.; Biroccio, A.; Ceccacci, A.; Pacini, L.; Narjes, F.; Gennari, N.; Bisbocci, M.; Incitti, I.; Orsatti, L.; Harper, S.; Stansfield, I.; Rowley, M.; De Francesco, R.; Migliaccio, G. Mechanism of Action and Antiviral Activity of Benzimidazole-Based Allosteric Inhibitors of the Hepatitis C Virus RNA-Dependent RNA Polymerase. *Journal of Virology* **2003**, *77*, 13225-13231, https://doi.org/10.1128/JVI.77.24.13225-13231.2003.
31. Narayanaswamy, V.K.; Rissdörfer, M.; Odhav, B. Review on CambridgeSoft ChemBioDraw Ultra 13.0v. *International Journal of theoretical & applied sciences* **2013**, *5*, 45-49.
32. Halgren, T.A. Merck molecular force field. I. Basis, form, scope, parameterization, and performance of MMFF94. *Journal of computational chemistry* **1996**, *17*, 490-519, https://doi.org/10.1002/(SICI)1096-987X(199604)17:5/6%3C490::AID-JCC1%3E3.0.CO;2-P.
33. Hanwell, M.D.; Curtis, D.E.; Lonie, D.C.; Vandermeersch, T.; Zurek, E.; Hutchison, G.R. Avogadro: an advanced semantic chemical editor, visualization, and analysis platform. *Journal of cheminformatics* **2012**, *4*, 17, https://doi.org/10.1186/1758-2946-4-17.
34. Cheng, F.; Li, W.; Liu, G.; Tang, Y. *In silico* ADMET prediction: recent advances, current challenges and future trends. *Current topics in medicinal chemistry* **2013**, *13*, 1273-1289, https://www.doi.org/10.2174/15680266113139990033.
35. Hanee, U.; Rahman, M.; Matin, M.M. Synthesis, PASS, *In silico* ADMET and Thermodynamic Studies of Some Galactopyranoside Esters. *Physical Chemistry Research* **2021**, *9*, 591-603, https://dx.doi.org/10.22036/pcr.2021.282956.1911.
36. Matin, M.M.; Islam, N.; Siddika, A.; Bhattacharjee, S.C. Regioselective synthesis of some rhamnopyranoside esters for PASS predication, and ADMET studies. *Journal of the Turkish Chemical Society Section A: Chemistry* **2021**, *8*, 365-374, https://doi.org/10.18596/jotcsa.829658.
37. Daina, A.; Michielin, O.; Zoete, V. SwissADME: a free web tool to evaluate pharmacokinetics, drug-likeness and medicinal chemistry friendliness of small molecules. *Scientific reports* **2017**, *7*, 42717, https://doi.org/10.1038/srep42717.
38. Banerjee, P.; Eckert, A.O.; Schrey, A.K.; Preissner, R. ProTox-II: a webserver for the prediction of toxicity of chemicals. *Nucleic acids research* **2018**, *46*, W257-W263, https://doi.org/10.1093/nar/gky318.
39. Jones, G.; Willett, P.; Glen, R.C.; Leach, A.R.; Taylor, R. Development and validation of a genetic algorithm for flexible docking. *Journal of molecular biology* **1997**, *267*, 727-748, https://doi.org/10.1006/jmbi.1996.0897.
40. Elkamhawy, A.; Lee, J.; Park, B.G.; Park, I.; Pae, A.N.; Roh, E.J. Novel quinazoline-urea analogues as modulators for Aβ-induced mitochondrial dysfunction: Design, synthesis, and molecular docking study. *European journal of medicinal chemistry* **2014**, *84*, 466-475, https://doi.org/10.1016/j.ejmech.2014.07.027.

41. Atanasova, M.; Yordanov, N.; Dimitrov, I.; Berkov, S.; Doytchinova, I. Molecular docking study on galantamine derivatives as cholinesterase inhibitors. *Molecular informatics* **2015**, *34*, 394-403, https://doi.org/10.1002/minf.201400145.
42. Franco, L.S.; Maia, R.C.; Barreiro, E.J. Identification of LASSBio-1945 as an inhibitor of SARS-CoV-2 main protease ($M^{PRO}$) through *in silico* screening supported by molecular docking and a fragment-based pharmacophore model. *RSC medicinal chemistry* **2021**, *12*, 110-119, https://doi.org/10.1039/D0MD00282H.
43. Pawar, S.S.; Rohane, S.H. Review on Discovery Studio: An important Tool for Molecular Docking. *Asian Journal of Research in Chemistry* **2021**, *14*, 86-88, https://doi.org/10.5958/0974-4150.2021.00014.6.
44. Benet, L.Z.; Hosey, C.M.; Ursu, O.; Oprea, T.I. BDDCS, the rule of 5 and drugability. *Advanced drug delivery reviews* **2016**, *101*, 89-98, https://doi.org/10.1016/j.addr.2016.05.007.
45. Veber, D.F.; Johnson, S.R.; Cheng, H.Y.; Smith, B.R.; Ward, K.W.; Kopple, K.D. Molecular properties that influence the oral bioavailability of drug candidates. *Journal of medicinal chemistry* **2002**, *45*, 2615-2623, https://doi.org/10.1021/jm020017n.
46. Kavitha, N.; Alivelu, M.; Konakanchi, R. Computational Quantum Chemical Study, Insilco ADMET, and Molecular Docking Study of 2-Mercapto Benzimidazole. *Polycyclic Aromatic Compounds* **2021**, 1-16, https://doi.org/10.1080/10406638.2021.1939071.
47. Al-Masoudi, N.A.; Elias, R.S.; Saeed, B. Molecular Docking Studies of some Antiviral and Antimalarial Drugs Via Bindings to 3CL-Protease and Polymerase Enzymes of the Novel Coronavirus (SARS-CoV-2). *Biointerface Research in Applied Chemistry* **2020**, *10*, 6444-6459, https://doi.org/10.33263/BRIAC105.64446459.
48. Vallianou, N.G.; Tsilingiris, D.; Christodoulatos, G.S.; Karampela, I.; Dalamaga, M. Anti-viral treatment for SARS-CoV-2 infection: A race against time amidst the ongoing pandemic. *Metabolism open* **2021**, *10*, 100096, https://doi.org/10.1016/j.metop.2021.100096.
49. Benigni, R.; Bossa, C. Structural alerts of mutagens and carcinogens. *Current Computer-Aided Drug Design* **2006**, *2*, 169-176, https://doi.org/10.2174/157340906777441663.
50. Umbuzeiro, G.D.A.; Heringa, M.; Zeiger, E. *In vitro* genotoxicity testing: significance and use in environmental monitoring. *In: Reifferscheid G.; Buchinger S. (eds) In vitro Environmental Toxicology - Concepts, Application and Assessment. Advances in Biochemical Engineering/Biotechnology*, *157*, Springer, Cham **2016**, https://doi.org/10.1007/10_2015_5018.
51. Kauffmann, K.; Werner, F.; Deitert, A.; Finklenburg, J.; Brendt, J.; Schiwy, A.; Hollert, H.; Büchs, J. Optimization of the Ames RAMOS test allows for a reproducible high-throughput mutagenicity test. *Science of The Total Environment* **2020**, *717*, 137168, https://doi.org/10.1016/j.scitotenv.2020.137168.
52. Hrelia, P.; Morotti, M.; Vigagni, F.; Burnelli, S.; Garuti, L.; Sabatino, P.; Cantelli-Forti, G. Synthesis of a series of 5-nitro-(benzimidazoles and indoles) as novel antimycotics and evaluation as genotoxins in the Ames test. *Mutagenesis* **1993**, *8*, 183-188, https://doi.org/10.1093/mutage/8.3.183.
53. DeWitt, J.C.; Keil, D.E. Current Issues in Developmental Immunotoxicity. *In: Parker, G. (eds) Immunopathology in Toxicology and Drug Development. Molecular and Integrative Toxicology*, Humana Press, Cham **2017**, https://doi.org/10.1007/978-3-319-47377-2_13.
54. Aslantürk, Ö.S. *In vitro* cytotoxicity and cell viability assays: principles, advantages, and disadvantages. *In: Larramendy, M.L.; Soloneski, S. (eds) Genotoxicity - A predictable risk to our actual world*, IntechOpen Limited, London **2018**, UK, https://doi.org/10.5772/intechopen.71923.

# Supplementary materials

**Table S1.** Compound's Informations.

| Compound | CAS Number | Name |
|---|---|---|
| 1 | 1296275-70-1 | *N*-(4-(benzyloxy)phenyl)-2-((6-methoxy-1*H*-benzo[d]imidazol-2-yl)sulfinyl)acetamide |
| 2 | 1296275-72-3 | *N*-(4-(benzyloxy)phenyl)-2-((6-(difluoromethoxy)-1*H*-benzo[*d*]imidazol-2-yl)sulfinyl)acetamide |
| 3 | 491873-62-2 | 2-(((1*H*-benzo[*d*]imidazol-2-yl)thio)methyl)-5-(4-chlorophenyl)-1,3,4-oxadiazole |
| 4 | 1180392-64-6 | 2-(((1*H*-benzo[*d*]imidazol-2-yl)thio)methyl)-5-(3,4,5-trimethoxyphenyl)-1,3,4-oxadiazole |
| 5 | 1226777-40-7 | 2-(((1*H*-benzo[*d*]imidazol-2-yl)thio)methyl)-5-(2-chloro-4-nitrophenyl)-1,3,4-oxadiazole |
| 6 | 915159-42-1 | 2-((1*H*-benzo[*d*]imidazol-2-yl)thio)-*N*-(2-(4-chlorophenyl)-4-oxothiazolidin-3-yl)acetamide |
| 7 | 915159-35-2 | 2-((1*H*-benzo[*d*]imidazol-2-yl)thio)-*N*-(2-(2-hydroxyphenyl)-4-oxothiazolidin-3-yl)acetamide |
| 8 | 915159-37-4 | 2-((1*H*-benzo[*d*]imidazol-2-yl)thio)-*N*-(2-(4-hydroxyphenyl)-4-oxothiazolidin-3-yl)acetamide |
| 9 | 1381961-08-5 | (*E*)-2-(2-chlorostyryl)-3-(2-thioxo-2,3-dihydro-1*H*-benzo[d]imidazol-5-yl)quinazolin-4(3*H*)-one |
| 10 | 1381961-09-6 | (*E*)-2-(4-chlorostyryl)-3-(2-thioxo-2,3-dihydro-1*H*-benzo[d]imidazol-5-yl)quinazolin-4(3*H*)-one |
| 11 | 1381961-10-9 | (*E*)-2-(4-methoxystyryl)-3-(2-thioxo-2,3-dihydro-1*H*-benzo[d]imidazol-5-yl)quinazolin-4(3*H*)-one |
| 12 | 1315475-96-7 | 1-tosyl-2-(((1-tosyl-1*H*-benzo[d]imidazol-2-yl)methyl)thio)-1*H*-benzo[d]imidazole |
| 13 | 1415985-81-7 | (*E*)-2-((1*H*-benzo[d]imidazol-2-yl)thio)-*N*-(4-(3-(4-hydroxy-3-methoxyphenyl)acryloyl)phenyl)acetamide |
| 14 | 1415985-80-6 | (*E*)-2-((1*H*-benzo[d]imidazol-2-yl)thio)-*N*-(4-(3-(2,5-dimethoxyphenyl)acryloyl)phenyl)acetamide |
| 15 | 1415985-78-2 | (*E*)-2-((1*H*-benzo[*d*]imidazol-2-yl)thio)-*N*-(4-(3-(3,4,5-trimethoxyphenyl)acryloyl)phenyl)acetamide |
| 16 | 1415985-79-3 | (*E*)-2-((1*H*-benzo[d]imidazol-2-yl)thio)-*N*-(4-(3-(2-nitrophenyl)acryloyl)phenyl)acetamide |
| 17 | 1415985-83-9 | (*E*)-2-((1*H*-benzo[d]imidazol-2-yl)thio)-*N*-(4-(3-(2-hydroxyphenyl)acryloyl)phenyl)acetamide |
| 18 | 1686086-89-4 | (*E*)-2-((1*H*-benzo[d]imidazol-2-yl)thio)-*N*'-(4-((3-chlorobenzylidene)amino)-5-mercapto-4,5-dihydro-3*H*-1,2,4-triazol-3-yl)acetohydrazide |
| 19 | 1686087-98-8 | (*E*)-2-((1H-benzo[d]imidazol-2-yl)thio)-*N*'-(5-mercapto-4-((3-nitrobenzylidene)amino)-4,5-dihydro-3*H*-1,2,4-triazol-3-yl)acetohydrazide |
| 20 | 1824037-65-1 | 5-chloro-3-(6-phenyl-2-thioxo-1,2,3,5-tetrahydroimidazo[4,5-*f*]indol-7-yl)indolin-2-one |
| 21 | 1824037-68-4 | 3-(6-(4-bromophenyl)-2-thioxo-1,2,3,5-tetrahydroimidazo[4,5-*f*]indol-7-yl)indolin-2-one |
| 22 | 2363044-55-5 | 2-((1-benzoyl-1*H*-benzo[*d*]imidazol-2-yl)thio)-*N*-(2,5-dichlorophenyl)acetamide |

| Compound | CAS Number | Name |
|---|---|---|
| 23 | 2363044-56-6 | 2-((1-benzoyl-1*H*-benzo[*d*]imidazol-2-yl)thio)-*N*-(2-bromophenyl)acetamide |
| 24 | 2363044-57-7 | 2-((1-benzoyl-1*H*-benzo[*d*]imidazol-2-yl)thio)-*N*-(3-bromophenyl)acetamide |
| 25 | 2363044-58-8 | 2-((1-benzoyl-1*H*-benzo[*d*]imidazol-2-yl)thio)-*N*-(4-bromophenyl)acetamide |
| 26 | 2363044-60-2 | 2-((1-benzoyl-1*H*-benzo[d]imidazol-2-yl)thio)-*N*-(4-chloro-2-nitrophenyl)acetamide |
| 27 | 1610736-34-9 | 2'-(2-thioxo-2,3-dihydro-1*H*-benzo[*d*]imidazol-5-yl)-2',3'-dihydrospiro[indoline-3,1'-isoindole]-2,4',7'-trione |
| 28 | 1610736-36-1 | 5-(methoxymethyl)-2'-(2-thioxo-2,3-dihydro-1*H*-benzo[*d*]imidazol-5-yl)-2',3'-dihydrospiro[indoline-3,1'-isoindole]-2,4',7'-trione |
| 29 | 1610736-37-2 | 5-methyl-2'-(2-thioxo-2,3-dihydro-1*H*-benzo[*d*]imidazol-5-yl)-2',3'-dihydrospiro[indoline-3,1'-isoindole]-2,4',7'-trione |
| 30 | 1610736-38-3 | 5-bromo-2'-(2-thioxo-2,3-dihydro-1*H*-benzo[*d*]imidazol-5-yl)-2',3'-dihydrospiro[indoline-3,1'-isoindole]-2,4',7'-trione |
| 31 | 1610736-39-4 | 5-nitro-2'-(2-thioxo-2,3-dihydro-1*H*-benzo[*d*]imidazol-5-yl)-2',3'-dihydrospiro[indoline-3,1'-isoindole]-2,4',7'-trione |
| 32 | 2236048-91-0 | (*E*)-*N*'-(4-methylbenzylidene)-2-(2-(tetradecylthio)-1*H*-benzo[*d*]imidazol-1-yl)acetohydrazide |
| 33 | 2236048-92-1 | (*E*)-N'-(4-nitrobenzylidene)-2-(2-(tetradecylthio)-1*H*-benzo[*d*]imidazol-1-yl)acetohydrazide |
| 34 | 2236048-93-2 | (*E*)-2-(2-(tetradecylthio)-1*H*-benzo[*d*]imidazol-1-yl)-N'-(3,4,5-trimethoxybenzylidene)acetohydrazide |
| 35 | 2236048-94-3 | (*E*)-N'-(3-hydroxy-4-methoxybenzylidene)-2-(2-(tetradecylthio)-1*H*-benzo[*d*]imidazol-1-yl)acetohydrazide |
| 36 | 2236048-96-5 | (*E*)-N'-(4-chlorobenzylidene)-2-(2-(tetradecylthio)-1*H*-benzo[*d*]imidazol-1-yl)acetohydrazide |
| 37 | 2236048-97-6 | (*E*)-N'-(2-methylbenzylidene)-2-(2-(tetradecylthio)-1*H*-benzo[*d*]imidazol-1-yl)acetohydrazide |
| 38 | 2236048-98-7 | (*E*)-N'-(3,4-dimethoxybenzylidene)-2-(2-(tetradecylthio)-1*H*-benzo[*d*]imidazol-1-yl)acetohydrazide |
| 39 | 2236048-99-8 | (*E*)-N'-(2,4-dichlorobenzylidene)-2-(2-(tetradecylthio)-1*H*-benzo[*d*]imidazol-1-yl)acetohydrazide |
| 40 | 2236049-00-4 | (*E*)-N'-(4-formylbenzylidene)-2-(2-(tetradecylthio)-1*H*-benzo[*d*]imidazol-1-yl)acetohydrazide |
| 41 | 2236049-01-5 | (*E*)-N'-(4-methoxybenzylidene)-2-(2-(tetradecylthio)-1*H*-benzo[*d*]imidazol-1-yl)acetohydrazide |
| 42 | 2236049-02-6 | (*E*)-N'-(4-hydroxybenzylidene)-2-(2-(tetradecylthio)-1*H*-benzo[*d*]imidazol-1-yl)acetohydrazide |
| 43 | 2236049-03-7 | (*E*)-N'-(4-(methylthio)benzylidene)-2-(2-(tetradecylthio)-1*H*-benzo[*d*]imidazol-1-yl)acetohydrazide |
| 44 | 2236049-04-8 | (*E*)-N'-(4-(dimethylamino)benzylidene)-2-(2-(tetradecylthio)-1*H*-benzo[*d*]imidazol-1-yl)acetohydrazide |
| 45 | 2468196-61-2 | 1-(2-(methylthio)-1*H*-benzo[*d*]imidazol-1-yl)-3-phenylpropan-1-one |
| 46 | 2468196-65-6 | 3-phenyl-1-(2-(propylthio)-1*H*-benzo[*d*]imidazol-1-yl)propan-1-one |
| 47 | 2468196-67-8 | (*E*)-1-(2-(methylthio)-1*H*-benzo[*d*]imidazol-1-yl)-3-phenylprop-2-en-1-one |
| 48 | 2468196-69-0 | (*E*)-1-(2-(ethylthio)-1*H*-benzo[*d*]imidazol-1-yl)-3-phenylprop-2-en-1-one |
| 49 | 2468196-70-3 | (*E*)-3-phenyl-1-(2-(propylthio)-1*H*-benzo[*d*]imidazol-1-yl)prop-2-en-1-one |

| Compound | CAS Number | Name |
|---|---|---|
| 50 | 1322296-33-2 | (*E*)-3-(4-fluorophenyl)-1-(2-(methylthio)-1*H*-benzo[*d*]imidazol-1-yl)prop-2-en-1-one |
| 51 | 2468196-71-4 | (*E*)-1-(2-(ethylthio)-1*H*-benzo[*d*]imidazol-1-yl)-3-(4-fluorophenyl)prop-2-en-1-one |
| 52 | 2468196-73-6 | (*E*)-3-(4-fluorophenyl)-1-(2-(propylthio)-1*H*-benzo[*d*]imidazol-1-yl)prop-2-en-1-one |
| 53 | 2468196-75-8 | (*E*)-3-(4-chlorophenyl)-1-(2-(methylthio)-1*H*-benzo[*d*]imidazol-1-yl)prop-2-en-1-one |
| 54 | 2468196-77-0 | (*E*)-3-(4-chlorophenyl)-1-(2-(ethylthio)-1*H*-benzo[*d*]imidazol-1-yl)prop-2-en-1-one |
| 55 | 2468196-79-2 | (*E*)-3-(4-chlorophenyl)-1-(2-(propylthio)-1*H*-benzo[*d*]imidazol-1-yl)prop-2-en-1-one |
| 56 | 2468196-81-6 | (*E*)-3-(4-bromophenyl)-1-(2-(methylthio)-1*H*-benzo[*d*]imidazol-1-yl)prop-2-en-1-one |
| 57 | 2468196-83-8 | (*E*)-3-(4-bromophenyl)-1-(2-(ethylthio)-1*H*-benzo[*d*]imidazol-1-yl)prop-2-en-1-one |
| 58 | 2468196-85-0 | (*E*)-3-(4-bromophenyl)-1-(2-(propylthio)-1*H*-benzo[*d*]imidazol-1-yl)prop-2-en-1-one |
| 59 | 2468196-87-2 | 1-(2-(methylthio)-1*H*-benzo[*d*]imidazol-1-yl)-3-phenylprop-2-yn-1-one |
| 60 | 2468196-89-4 | 1-(2-(ethylthio)-1*H*-benzo[*d*]imidazol-1-yl)-3-phenylprop-2-yn-1-one |
| 61 | 2468196-91-8 | 3-phenyl-1-(2-(propylthio)-1*H*-benzo[*d*]imidazol-1-yl)prop-2-yn-1-one |

**Druglikeness Properties: http://www.swissadme.ch/**

**Table S2.** MW: Molecular weight; HBD: H-bond donors; HBA: H-bond acceptors; NRB: Num. rotatable bonds; TPSA: Topological polar surface area.

| Compound | MW (≤500) | HBD (≤5) | HBA (≤10) | cLOGP (≤5.00) | NRB (≤10) | TPSA (≤140) |
|---|---|---|---|---|---|---|
| **1** | 435.50 | 2 | 5 | 3.13 | 9 | 112.52 |
| **2** | 471.48 | 2 | 7 | 3.76 | 10 | 112.52 |
| **3** | 342.80 | 1 | 4 | 3.68 | 4 | 92.90 |
| **4** | 398.44 | 1 | 7 | 3.23 | 7 | 120.59 |
| **5** | 387.80 | 1 | 6 | 2.96 | 5 | 138.72 |
| **6** | 418.92 | 2 | 3 | 3.12 | 6 | 128.69 |
| **7** | 400.47 | 3 | 4 | 2.19 | 6 | **148.92** |
| **8** | 400.47 | 3 | 4 | 2.04 | 6 | **148.92** |
| **9** | 430.91 | 4 | 7 | 4.68 | 10 | 102.37 |
| **10** | 430.91 | 1 | 3 | 4.69 | 3 | 102.37 |
| **11** | 426.49 | 1 | 4 | 4.13 | 4 | 111.60 |
| **12** | **588.72** | 0 | 6 | **5.47** | 7 | **145.98** |
| **13** | 459.52 | 3 | 5 | 3.70 | 9 | 129.61 |
| **14** | 473.54 | 2 | 5 | 4.08 | 10 | 118.61 |
| **15** | 503.57 | 2 | 6 | 4.16 | 11 | 127.84 |
| **16** | 458.49 | 2 | 5 | 3.39 | 9 | **145.97** |
| **17** | 429.49 | 3 | 4 | 3.72 | 8 | 120.38 |
| **18** | 460.96 | 3 | 6 | 3.00 | 8 | **174.23** |
| **19** | 471.52 | 3 | 8 | 1.88 | 9 | **220.05** |
| **20** | 430.91 | 3 | 2 | 4.31 | 2 | 112.37 |
| **21** | 475.36 | 2 | 2 | 4.48 | 3 | 112.37 |
| **22** | 456.34 | 1 | 3 | 4.83 | 7 | 89.29 |
| **23** | 466.35 | 1 | 3 | 4.39 | 7 | 89.29 |
| **24** | 466.35 | 1 | 3 | 4.32 | 7 | 89.29 |
| **25** | 466.35 | 1 | 3 | 4.32 | 7 | 89.29 |
| **26** | 466.90 | 1 | 5 | 3.76 | 8 | 135.11 |

| Compound | MW (≤500) | HBD (≤5) | HBA (≤10) | cLOGP (≤5.00) | NRB (≤10) | TPSA (≤140) |
|---|---|---|---|---|---|---|
| **27** | 414.44 | 2 | 4 | 1.88 | 1 | 133.96 |
| **28** | 444.46 | 2 | 5 | 1.88 | 2 | **143.19** |
| **29** | 428.46 | 2 | 4 | 2.22 | 1 | 133.96 |
| **30** | 493.33 | 2 | 4 | 2.47 | 1 | 133.96 |
| **31** | 459.43 | 2 | 6 | 1.13 | 2 | **179.78** |
| **32** | **520.77** | 1 | 3 | **7.72** | **19** | 84.58 |
| **33** | **551.74** | 1 | 5 | **6.50** | **20** | 130.40 |
| **34** | **596.82** | 1 | 6 | **7.30** | **22** | 112.27 |
| **35** | **552.77** | 2 | 5 | **6.98** | **20** | 114.04 |
| **36** | **541.19** | 1 | 3 | **7.91** | **19** | 84.58 |
| **37** | **520.77** | 1 | 3 | **7.60** | **19** | 84.58 |
| **38** | **566.80** | 1 | 5 | **7.31** | **21** | 103.04 |
| **39** | **575.64** | 1 | 3 | **8.42** | **19** | 84.58 |
| **40** | **534.76** | 1 | 4 | **7.01** | **20** | 101.65 |
| **41** | **536.77** | 1 | 4 | **7.28** | **20** | 93.81 |
| **42** | **522.75** | 2 | 4 | **6.98** | **19** | 104.81 |
| **43** | **552.84** | 1 | 3 | **7.86** | **20** | 109.88 |
| **44** | **549.81** | 1 | 3 | **7.28** | **20** | 87.82 |
| **45** | 296.39 | 0 | 2 | 3.70 | 5 | 60.19 |
| **46** | 324.44 | 0 | 2 | 4.37 | 7 | 60.19 |
| **47** | 294.37 | 0 | 2 | 3.69 | 4 | 60.19 |
| **48** | 308.40 | 0 | 2 | 3.99 | 5 | 60.19 |
| **49** | 322.42 | 0 | 2 | 4.36 | 6 | 60.19 |
| **50** | 312.36 | 0 | 3 | 4.01 | 4 | 60.19 |
| **51** | 326.39 | 0 | 3 | 4.33 | 5 | 60.19 |
| **52** | 340.41 | 0 | 3 | 4.66 | 6 | 60.19 |
| **53** | 328.82 | 0 | 2 | 4.21 | 4 | 60.19 |
| **54** | 342.84 | 0 | 2 | 4.52 | 5 | 60.19 |
| **55** | 356.87 | 0 | 2 | 4.90 | 6 | 60.19 |
| **56** | 373.27 | 0 | 2 | 4.30 | 4 | 60.19 |
| **57** | 387.29 | 0 | 2 | 4.60 | 5 | 60.19 |
| **58** | 401.32 | 0 | 2 | 4.98 | 6 | 60.19 |
| **59** | 292.35 | 2 | 2 | 3.60 | 0 | 60.19 |
| **60** | 306.38 | 0 | 2 | 3.91 | 3 | 60.19 |
| **61** | 320.41 | 0 | 2 | 4.28 | 4 | 60.19 |

Violate Lipinski and/or Veber rules

**Table S3.** Docking Scores by Gold.

| Compound | ASP.Fitness score | Compound | ASP.Fitness score | Compound | ASP.Fitness score |
|---|---|---|---|---|---|
| **1** | 45.33 | **23** | 38.70 | **45** | 33.03 |
| **2** | **48.64** | **24** | 38.32 | **46** | 35.78 |
| **3** | 34.52 | **25** | 37.97 | **47** | 31.15 |
| **4** | 38.68 | **26** | 33.37 | **48** | 32.72 |
| **5** | 39.94 | **27** | 33.17 | **49** | 33.00 |
| **6** | 34.01 | **28** | 35.30 | **50** | 33.67 |
| **7** | - | **29** | 33.49 | **51** | 33.44 |
| **8** | - | **30** | 33.43 | **52** | 34.78 |
| **9** | 38.30 | **31** | - | **53** | 33.66 |
| **10** | 38.55 | **32** | - | **54** | 33.68 |
| **11** | 38.65 | **33** | - | **55** | 34.58 |
| **12** | - | **34** | - | **56** | 33.73 |
| **13** | **49.00** | **35** | - | **57** | 33.83 |

| Compound | ASP.Fitness score | Compound | ASP.Fitness score | Compound | ASP.Fitness score |
|---|---|---|---|---|---|
| **14** | 47.69 | **36** | - | **58** | 34.76 |
| **15** | - | **37** | - | **59** | 32.56 |
| **16** | - | **38** | - | **60** | 32.98 |
| **17** | **47.94** | **39** | - | **61** | 31.94 |
| **18** | - | **40** | - | Remdesivir | 36.37 |
| **19** | - | **41** | - | Umifenovir | 33.30 |
| **20** | 40.39 | **42** | - | | |
| **21** | 39.95 | **43** | - | | |
| **22** | 40.10 | **44** | - | | |